Research Article

Lulu Zhang*, Jing Wang, and Qingyi Wang

Influence of pH on the synthesis of carbon spheres and the application of carbon spherebased solid catalysts in esterification

https://doi.org/10.1515/rams-2024-0060 received June 30, 2024; accepted September 20, 2024

Abstract: Size uniformity is a key challenge in the preparation of hydrothermal carbon spheres and a prerequisite for size effect research and many applications of carbon spheres. To solve the scientific problem of low uniformity due to the slow carbonization in traditional preparation of glucose carbon spheres, we propose to add acid/base catalysts to accelerate nucleation, shorten the nucleation time, and improve the size uniformity of carbon spheres. The carbon spheres prepared under base conditions versus acid conditions have higher uniformity and smaller particle size (particle size = 503 nm). This result is due to the faster accumulation of aromatic clusters, shorter nucleation time, and larger number of carbon spheres in alkaline systems. The NaOH-HCSs-based solid acid catalyst as-prepared exhibits excellent catalytic activity, and the esterification rates of levulinic acid and *n*-butanol maximize to 96.36%.

Keywords: hydrothermal carbon spheres, acid/base catalysts, size uniformity, solid acid catalyst, biodiesel

1 Introduction

Carbon sphere is a new member of carbon nanomaterials after fullerenes, carbon nanotubes, and graphene. A spherical shape is the shape adopted by materials during synthesis (nucleation, growth) and is determined by considerations of energy minimization [1]. Compared with other types of carbon nanomaterials, the preparation process of carbon spheres is simpler. Among them, the hydrothermal method for preparing carbon spheres has the advantages of being green, sustainable, low-cost, and rich in surface functional groups [2]. Hydrothermal carbon spheres (HCSs) are nanomaterials with regular spherical morphology and are widely applied in chromatography [3], catalyst supports [4–6], hard template [7,8], reinforcement materials for rubber [9], biomedicines [10,11], and so forth. However, the size nonuniformity of HCSs is the key and difficulty in the preparation of carbon spheres. With glucose as an example, its hydrothermal carbonization to form carbon spheres conforms to the Lamer mechanism [12]. Specifically, water ionizes H⁺ and OH⁻, which act as acid and base catalysts, respectively, to catalyze glucose decomposition into 5-hydroxymethyl furfural (HMF) [13,14], organic acids (e.g., acetic acid, lactic acid, acrylic acid, levulinic acid (LA), formic acid), and other compounds (e.g., furfural, 1,2,4-benzenetriol) [15,16]. The organic acids formed during the hydrothermal process will act as acid catalysts to accelerate glucose decomposition. The HMF formed therefrom generates aromatic clusters through dehydration-condensation-polymerization. When the concentration of aromatic clusters reaches the critical supersaturation point, they explode into carbon nucleus, which then grow into carbon spheres each with a hydrophobic nuclei and a hydrophilic shell by enriching small molecules in the solution (HMF, LA, etc.) [17].

Reviews on Advanced Materials Science 2024: 63: 20240060

The HMF-generating rate in conventional hydrothermal carbonization of glucose is slow, resulting in a slow generation rate of aromatic clusters. When the concentration of aromatic clusters reaches the critical supersaturation point for the first time, carbon nuclei are generated and then

^{*} Corresponding author: Lulu Zhang, Technology Innovation Center for Land Engineering and Human Settlements, Shaanxi Land Engineering Construction Group Co., Ltd and Xi'an Jiaotong University, Xi'an, 710075, China; Shaanxi Provincial Land Engineering Construction Group, Land Engineering Technology Innovation Center, Ministry of Natural Resources, Xi'an, 710075, China; Institute of Land Engineering and Technology, Shaanxi Provincial Land Engineering Construction Group Co., Ltd, Xi'an, 710075, China; Shaanxi Dijian Land Engineering Quality Testing Co., Ltd, Xi'an, 710075, China, e-mail: lucy.20062008@163.com Jing Wang: Technology Innovation Center for Land Engineering and Human Settlements, Shaanxi Land Engineering Construction Group Co., Ltd and Xi'an Jiaotong University, Xi'an, 710075, China; Shaanxi Provincial Land Engineering Construction Group, Land Engineering Technology Innovation Center, Ministry of Natural Resources, Xi'an, 710075, China; Institute of Land Engineering and Technology, Shaanxi Provincial Land Engineering Construction Group Co., Ltd, Xi'an, 710075, China; Shaanxi Dijian Land Engineering Quality Testing Co., Ltd, Xi'an, 710075, China Qingyi Wang: Shaanxi Environmental Protection Innovation Center Co., Ltd, Xi'an, 712046, China

enriched with small molecules to form carbon spheres [18]. Then, HMF continues to generate aromatic clusters. After the concentration of aromatic clusters reaches the critical supersaturation point for the second time, they explode to form new carbon nuclei [19,20]. The time difference between the two times of carbon nucleolus generation will lead to size inhomogeneity in the carbon spheres. Therefore, accelerating the hydrothermal glucose carbonization and shortening the nucleation time of carbon spheres are the key factors in improving the size uniformity of carbon spheres. Since H⁺ and OH⁻ produced from water ionization are catalysts to promote glucose decomposition [21], adding acids or bases to increase the initial catalyst dosage may accelerate glucose carbonization.

Sobczuk et al. found [22] that pH has a significant impact on the diameter of carbon spheres prepared by the microwave heating solvothermal method. The diameters of carbon spheres obtained at the lowest pH value (7.50) and the highest pH value (10.00) were 780-920 nm and 80-150 nm, respectively, indicating that the diameter of carbon spheres decreases with increasing pH. Zhao et al. found [23] that the larger the amount of sulfuric acid added during the preparation of carbon spheres by hydrothermal method, the smaller the diameter of the carbon spheres. As sulfuric acid to water is 1:5, the diameter of carbon spheres is between 5 and 8 µm. As sulfuric acid to water is 1:2, the diameter range decreases to 1-4 µm. As the sulfuric acid ratio increases to 1:1, the diameter of carbon spheres decreases to within 100 nm. Réti et al. found [8] that when using sucrose as raw material and hydrothermal carbonization to prepare carbon spheres, the initial solution pH was 3, and the particle size distribution was wide, with an average particle size of 810 nm. When the initial pH is 12, the particle size distribution narrows and the average particle size is around 400 nm. Although there have been many studies on the effect of pH on carbon spheres, more attention has been paid to the analysis of pH on the morphology and particle size of carbon spheres, but systematic mechanism studies are still lacking.

In this study, we tried to increase the catalyst content in the initial glucose solution by adding HCl or NaOH as an acid or base catalyst and study the effects of different catalysts and pH on the glucose carbonization rate, and the size and uniformity of carbon spheres. The carbon spheres as-obtained were further carbonized and sulfonated to form solid acid catalysts, and their effect on the synthesis of biodiesel butyl levulinate (BL) was studied.

2 Experimental

2.1 Materials

Glucose, LA, n-butanol, and BL were all purchased from Aladdin. Hydrochloric acid (HCl), sodium hydroxide (NaOH), and sulfuric acid (H₂SO₄) were all bought from Sinopharm Chemical Reagent Co., Ltd.

2.2 Preparation of traditional hydrothermal carbon spheres (THCSs)

Glucose (10 g) was dissolved in 100 mL of deionized water and stirred for a few minutes to form a homogeneous solution. The homogeneous solution was transferred to a 200 mL corrosion-resistant autoclave. Then, the autoclave was heated at 6°C·min⁻¹ to 180°C, kept for 3 or 6 h, and then cooled naturally to room temperature. The carbon material was washed three times with deionized water and ethanol by repeated centrifugation/ultrasonic dispersion, and the resulting product was THCS.

2.3 Preparation of carbon spheres in HCl system (HCl-HCSs) or NaOH system (NaOH-HCSs)

Glucose (10 g) was dissolved in 100 mL of an HCl aqueous solution (pH = 3 or 4) and stirred for 15 min to form a homogeneous solution. The homogeneous solution was transferred to a 200 mL corrosion-resistant autoclave. Then, the autoclave was heated at 6° C·min⁻¹ to 180°C, kept for 3 or 6 h, and then cooled naturally to room temperature. The carbon material was three times with deionized water and ethanol by repeated centrifugation/ultrasonic dispersion, and the resulting product was HCl-HCS. In the same way, the pH of the solution was adjusted to 10 or 11, and the product was NaOH-HCS.

2.4 Preparation of carbon sphere-based solid acid catalysts

The carbon spheres were first carbonized at 600°C to improve their mechanical strength and catalytic stability as catalysts. With NaOH-HCSs as an example, NaOH-HCSs

(2 g) were placed in a 50 mL quartz boat. Then, the quartz boat was placed in a tube furnace, protected with nitrogen, and heated to 600°C at a heating rate of 10°C·min⁻¹. Carbonized NaOH-HCSs were obtained after keeping the temperature constant for 2 h.

Then, 1 g of the carbonized NaOH-HCSs and 10 mL of 98 wt% $\rm H_2SO_4$ were stirred evenly and transferred to a 25 mL hydrothermal autoclave lined. The autoclave was placed in an oven at 120°C for 10 h and then quickly cooled to room temperature [24]. The resulting solid acid catalyst was repeatedly washed with deionized water until no $\rm SO_4^{2-}$ was detected in the solution (Figure 1(a)).

2.5 Catalytic activity

The esterification reaction of LA and n-butanol was used as a probe reaction for analyzing catalyst activity (Figure 1(b)). LA (1.16 g), 4.44 g of n-butanol, and a certain amount (1, 5, 10 or 15 wt%) of the catalyst were put into a pressure bottle and reacted at a certain temperature (60, 80, 100 or 120°C) with a stirring speed of 200 r·min $^{-1}$ for 3 h. After the reaction, the mixture was quickly cooled in cold water. The yield of BL was calculated as follows:

$$BL_{vield}(\%) = BL/(LA0 \times 1.4827),$$
 (1)

where BL is the actual concentration of BL after the reaction; LA_0 is the initial concentration of LA; 1.4827 is the ratio of molecular weight of BL (172) to molecular weight of LA (116); $LA_0 \times 1.4827$ denotes that all LA_0 is converted to the theoretical concentration of BL.

2.6 Testing and characterization

The surface functional groups of carbon spheres were characterized on a Vertex 70 Fourier transform infrared spectrometer (FT-IR, Bruker, Germany) *via* KBr pellets and at 400–4,000 cm⁻¹. The crystallinity of carbon spheres were



Figure 1: (a) preparation of carbon sphere-based solid acid catalyst and (b) esterification of LA and *n*-butanol.

analyzed on a D8 Advance X-ray diffractometer (XRD, Bruker, Germany) with Cu-K α (1.5406 Å) as the radiation source and a scanning range of 2θ = 10° – 70° . The morphology of the carbon spheres was observed using a VEGA 3 EasyProbe scanning electron microscope (Scanning electron microscopy (SEM), TESCAN, Czech Republic). The element contents on the sample surface were analyzed using an energy-dispersive spectrometer (EDS, TESCAN, Czech Republic). The particle size distributions of the carbon spheres were analyzed with Nano Measurer 1.2 software. The specific surface area and pore structure of carbon spheres were analyzed using an ASAP 2460 N_2 adsorption desorption instrument (BET, Micromeritics, USA). The esterification reaction products were quantitatively analyzed with a GC-2014 device (Shimadzu, Japan).

3 Results and discussion

3.1 Morphology and particle size distribution of glucose-derived carbon spheres prepared from different hydrothermal methods

3.1.1 Traditional hydrothermal method

SEM shows the average particle size of THCSs increases with the extension of carbonization time from 169 nm after 3 h to 537 nm after 6 h (Figure 2), indicating the carbon nucleus as-generated continuously adsorbs the surrounding small organic molecules and gradually grows, which is consistent with previous studies [25,26]. The particle size distribution of the carbon spheres becomes wider with time – the reason is that the slow glucose carbonization rate in the traditional hydrothermal method makes the sphere nucleation time too long. Namely, the former carbon nuclei are always accompanied by the newly generated carbon nuclei during the growth. The carbon nuclei generated at different time points have different growth periods, which ultimately leads to low size uniformity of carbon spheres (Figure 3). Thus, accelerating glucose carbonization and shortening the nucleation time of carbon spheres may be the keys to solving this scientific problem.

3.1.2 Acidic system (HCl)

The effects of pH on the morphology and particle size of carbon spheres in a hydrochloric acid system (HCl-HCSs)

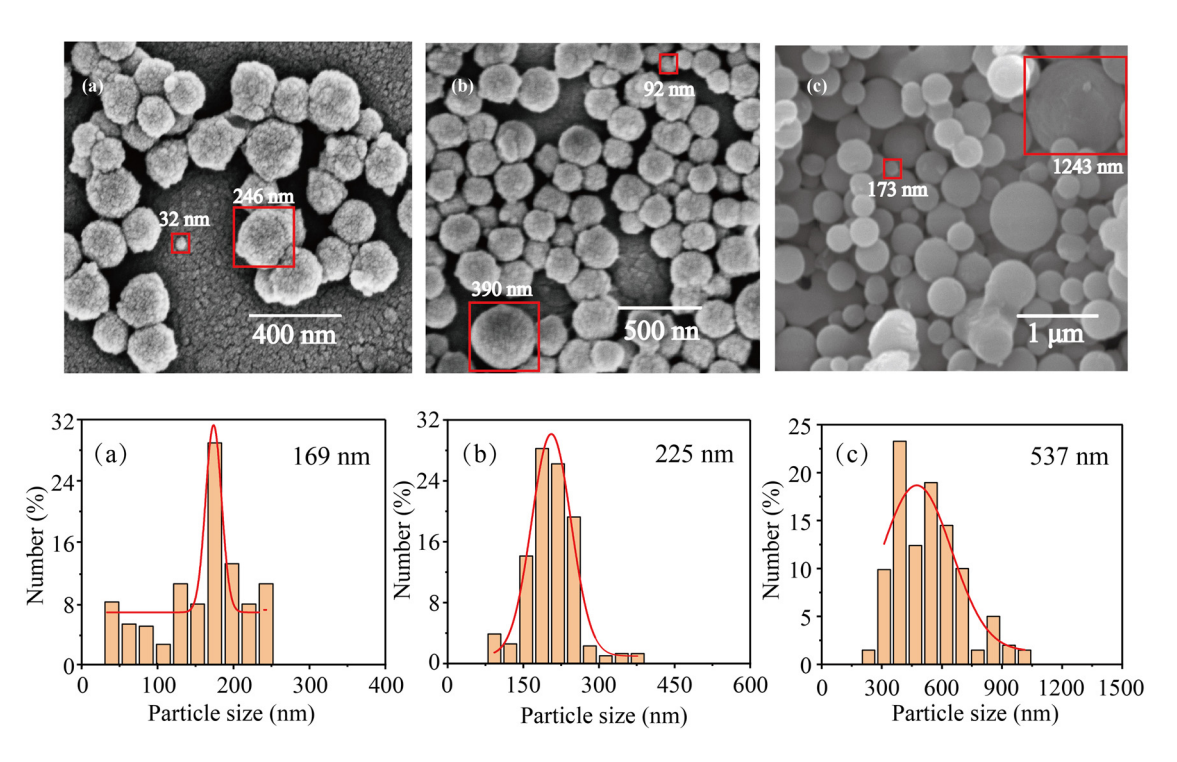


Figure 2: SEM images of THCSs: (A) and (a) 3.0 h; (B) and (b) 4.5 h; (C) and (c) 6.0 h.

were investigated with the presence of $0.5\,\mathrm{M}$ glucose and at $180^{\circ}\mathrm{C}$. The addition of HCl into the glucose carbonization system maintained the spherical morphology of the carbon spheres and significantly improved the size uniformity (Figure 4). These results indicate that the effect of pH on the uniformity of carbon spheres in an acidic system is particularly important. The effect on improving the uniformity of carbon spheres is better at pH = 4 than at pH = 3.

SEM showed that the average particle sizes of the carbon spheres prepared after 3 and 6 h are 408 and 651 nm, respectively, at pH = 3, but are 244 and 571 nm, respectively, at pH = 4. Namely, the particle sizes of the carbon spheres are smaller at pH = 4, indicating that pH affects the particle size of carbon spheres in addition to size uniformity. The reason may be that the acidity of the initial glucose solution is too high at pH = 3. Acidic conditions are favorable for glucose dehydration to generate HMF [27], but unfavorable for aldol reactions of cyclic and aromatic ketones/aldehydes, resulting in slow formation of aromatic

clusters and prolonged nucleation periods [28]. Therefore, the particle size and distribution of carbon spheres at pH = 3 are larger than those at pH = 4.

3.1.3 Base system (NaOH)

The effects of pH on the morphology and particle size of carbon spheres in a base system (NaOH-HCSs) were investigated in the presence of 0.5 M glucose and at 180°C. The addition of NaOH into the glucose carbonization system maintained the spherical morphology of the carbon spheres and improved size uniformity (Figure 5). Compared with the acidic systems, the base systems more largely affect the size uniformity of carbon spheres. The reason is that glucose is first dehydrated to HMF and then participates in polymerization and aldol condensation reactions to form aromatic clusters. In alkaline systems, the aldol reaction between cyclic ketones and aromatic ketones/aldehydes is more

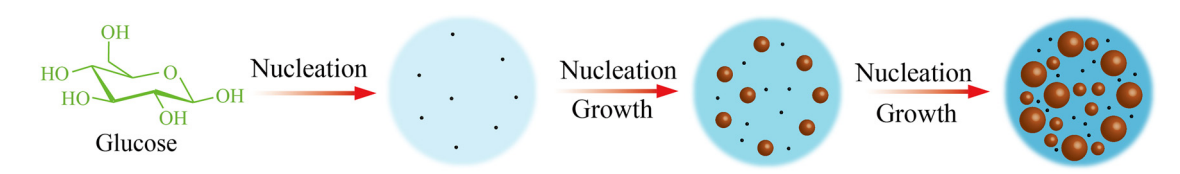


Figure 3: Schematic diagram of nucleation and nuclear growth of glucose-derived carbon spheres prepared by traditional hydrothermal method.

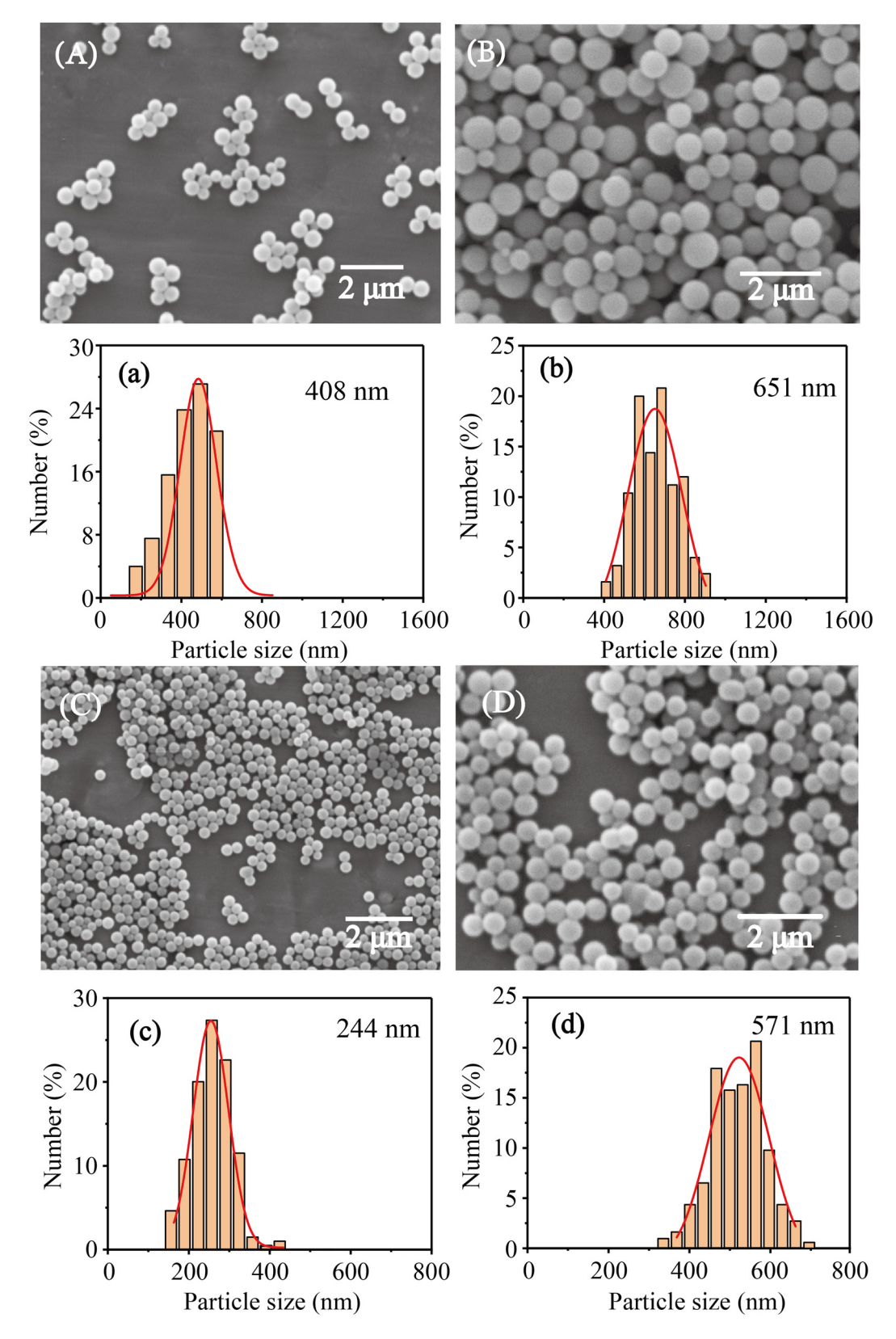


Figure 4: Typical SEM images of HCI-HCSs: (A) and (a) pH = 3, 3 h; (B) and (b) pH = 3, 6 h; (C) and (c) pH = 4, 3 h; (D) and (d) pH = 4, 6 h.

6 — Lulu Zhang et al. DE GRUYTER

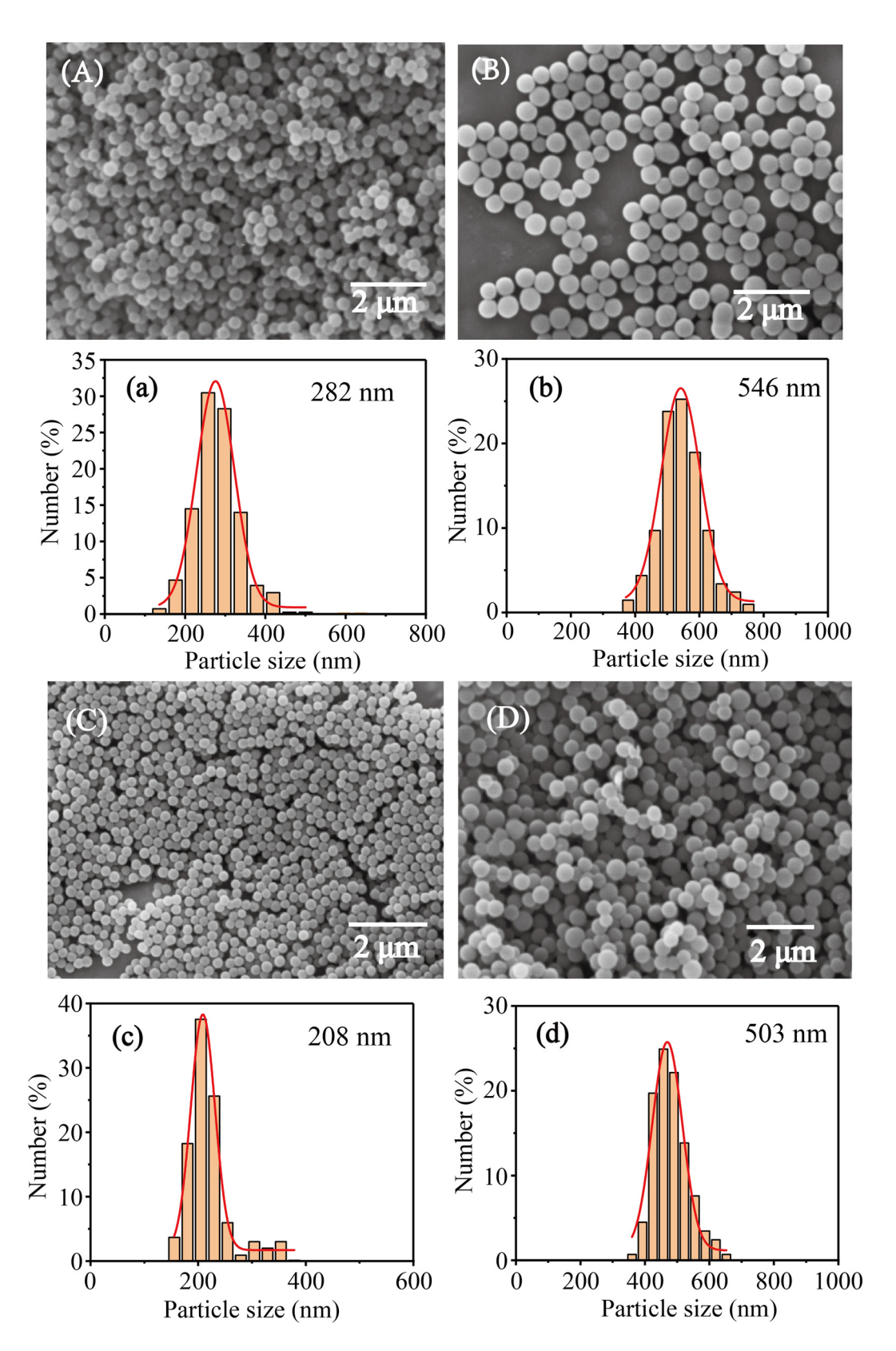


Figure 5: Typical SEM images of NaOH-HCSs: (A) and (a) pH = 10, 3 h; (B) and (b) pH = 10, 6 h; (C) and (c) pH = 11, 3 h; (D) and (d) pH = 11, 6 h.

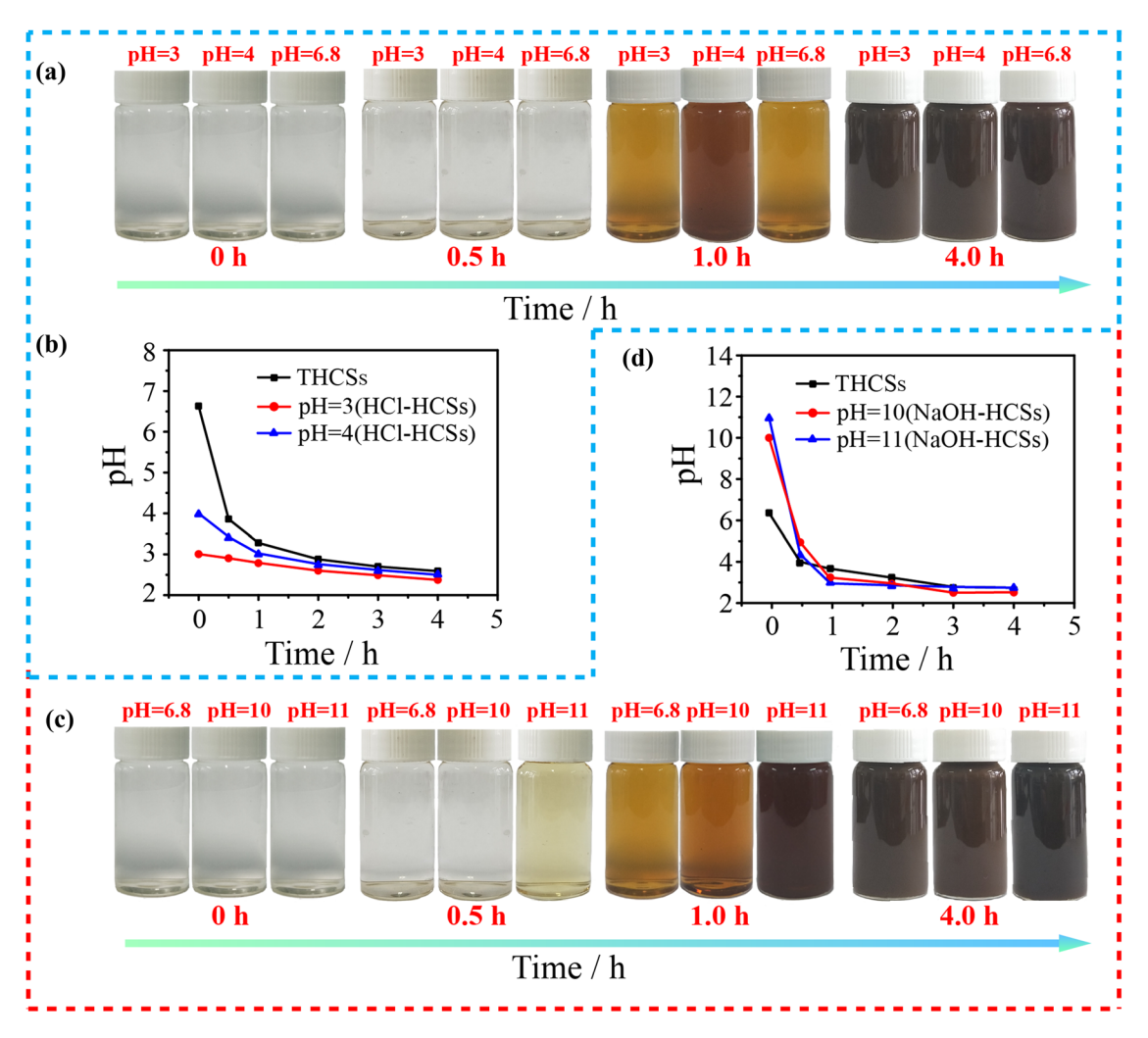


Figure 6: (a) Schematic diagram of hydrothermal carbonization in HCl system and neutral system; (b) pH changes with time in HCl system and neutral system; (c) Schematic diagram of hydrothermal carbonization in NaOH system and neutral system; (d) pH changes with time in NaOH system and neutral system.

favorable, which accelerates the accumulation of aromatic clusters and quickens nucleation after reaching the critical supersaturation point [29]. The shortened nucleation time significantly improves the uniformity of carbon spheres.

SEM showed that at pH = 11, the particle sizes of carbon spheres prepared after 3 or 6 h are smaller than those prepared at pH = 10, indicating the pH in the base systems also very critically influences the particle size of carbon spheres. Comparison shows that the NaOH-HCSs are smaller in particle size than the HCl-HCSs. The reason is that the nucleation time is shortened in the base systems, and due to the limitation of the total amount of raw materials, more raw materials are used for nucleation rather than nucleolus growth. Therefore, the particle sizes of NaOH-HCSs are smaller than those of the HCl-HCSs.

3.1.4 Effect of acid/base system on glucose carbonization rate

To verify that the addition of acid or base can accelerate glucose carbonization and shorten the nucleation time, we investigated the effects of HCl (Figure 6(a) and (b)) and NaOH (Figure 6(c) and (d)) on hydrothermal glucose carbonization rate and the pH decreasing rate.

Glucose solution is colorless and transparent, while carbon spheres are black brown in color. During glucose carbonization, the glucose solution gradually changed from being colorless and transparent to dark. Namely, the carbonization process can be visually observed from the color change of the glucose solution. Figure 6(a) shows the color change of glucose solutions with time at pH = 3, 4, and 6.8 (neutral). When the

initial solution was neutral, the color of the glucose solution changed slowly, indicating its carbonization rate was slow. In contrast, the addition of HCl significantly accelerated the blackening of the solution, especially at pH = 4, which verifies that HCl can accelerate glucose carbonization. The carbonization rate at pH = 3 was slower than that at pH = 4, which may be because excessive acids inhibit the carbonization rate [30]. The glucose carbonization will generate various organic acids, which act as new acid catalysts to further catalyze the glucose decomposition. Therefore, the speed of pH drop implies the glucose carbonization rate. Figure 6(b) illustrates the change in aqueous pH over time. When the initial solution was neutral. the pH decreases slowly, indicating that only small amounts of various organic acids were generated from the glucose decomposition, which means that the glucose carbonization was slow. The addition of HCl significantly accelerated the pH drop, which was caused by two reasons. First, the pH of the initial solution is low. Second, HCl accelerates glucose decomposition to produce organic acids. The rapidly generated organic acids further accelerate the glucose decomposition, verifying that the glucose carbonization rate is faster in an acidic system.

Figure 6(a) shows the color change of glucose solutions with time at pH = 6.8 (neutral), 10, and 11. Compared with THCSs, the glucose carbonization was significantly accelerated by the addition of NaOH and was the fastest at pH = 11. Compared with HCl-HCSs, the base systems more severely impacted the carbonization rate, which is consistent with the aforementioned results about the effect of acid/base systems on the uniformity and size of carbon spheres. Figure 6(d) illustrates the change of aqueous pH over time. In base systems, the base acted as a catalyst to accelerate glucose decomposition to produce organic acids. The organic acids then neutralized the base, eventually making the solution acidic. After 1h of hydrothermal carbonization, the pH of

the initial base systems was lower, which also verifies that the base catalyst can accelerate glucose carbonization.

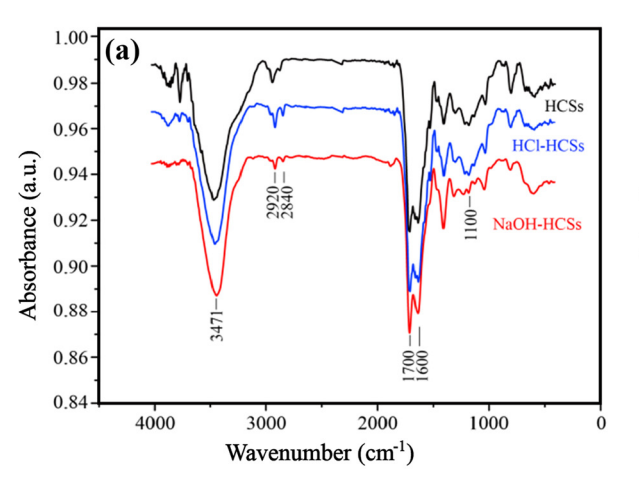
The chemical structures of THCSs, HCl-HCSs, and NaOH-HCSs were studied using fourier transform infrared (FTIR) and XRD. The characteristic peaks at 3,471 and 1,107 cm⁻¹ are due to OH stretching vibration and bending vibration, respectively; the peaks at 2,923 and 2,856 cm⁻¹ are characteristic of aliphatic –CH– stretching vibration, and the peaks at 700 and 1,625 cm⁻¹ correspond to C=O and C=C stretching vibration (Figure 7(a)) [31]. The infrared analysis shows a large number of oxygen-containing functional groups (OH⁻, –C=O, –COOH) on the surface of carbon spheres. Comparison of the FTIR spectra between HCl-HCSs and NaOH-HCSs indicates that the addition of acid/base catalysts does not change the types of surface functional groups in the carbon spheres.

The XRD spectra are shown in Figure 7(b). The peak at 2θ = 15°–30° belongs to the (002) crystal plane, indicating that the carbon material is composed of amorphous polycyclic aromatic carbon sheets. The weaker peak at 2θ = 40°–45° belongs to the (101) crystal plane, suggesting that the graphitization degree of the carbon material as-prepared is very low [32]. Comparison of XRD spectra between HCl-HCSs and NaOH-HCSs shows that the addition of acid/base catalysts will not affect the crystallinity of carbon spheres.

3.2 Performance of carbon sphere-based solid acid catalysts

3.2.1 Preparation and physicochemical properties of carbon sphere-based solid acid catalysts

The carbon spheres prepared from direct hydrothermal treatment of glucose are soft with a slight structural order.



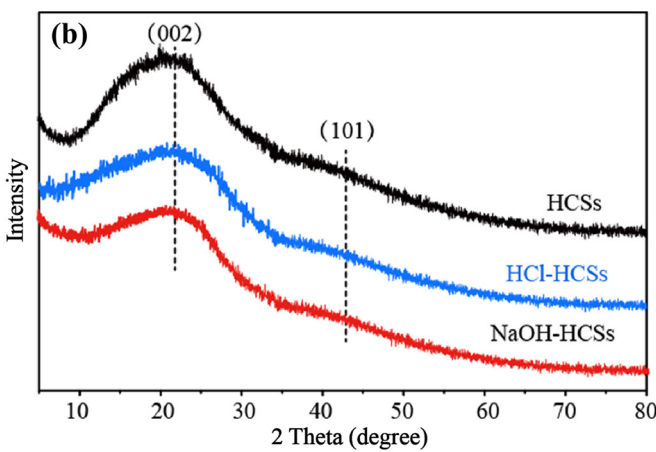


Figure 7: (a) FTIR spectrum and (b) XRD pattern of HCSs, HCI-HCSs and NaOH-HCSs.

The carbon spheres were first carbonized at high temperature to improve their mechanical strength and catalytic stability before the use as catalysts [33]. The influence of carbonization on the morphology, specific surface area, and pore structure of NaOH-HCSs was investigated with NaOH-HCSs as an example.

Figure 8(a) shows the SEM image of NaOH-HCSs after carbonization. The morphology of the carbonized carbon spheres is not changed significantly, and the original uniformity is maintained compared with Figure 5(b). After carbonization, the diameter of carbon spheres decreases. On the one hand, the escape of small-molecule substances generated during the carbonization process leads to a decrease in the total volume of carbon spheres. On the other hand, the carbonization process is accompanied by the reorganization and rearrangement of chemical bonds. The newly formed carbon-carbon bonds may make the structure of the carbon spheres more compact, further leading to a reduction in diameter [34]. XRD demonstrates that the (002) crystal plane peak becomes sharper and moves to a larger angle after carbonization, indicating that the spacing between carbon sheets is reduced, and namely, the graphitization degree is improved. The (101) crystal plane also moves to a larger angle and becomes sharper, indicating that the graphitization degree of the carbon spheres increases after carbonization [35]. The carbon content of the carbon spheres increases from 51 to 79% after carbonization, further indicating the increase in the carbonization degree.

Figure S1(a) and (c) shows a non-porous isotherm, indicating that there is no microporous and mesoporous structure. Figure S1(b) and (d) shows that the hysteresis loop belongs to type H4 loop, and the adsorption branch is composite of Types I and II [36], indicating that carbonized

carbon spheres have microporous and mesoporous structures. As can be seen from Table S1, the BET of NaOH-HCSs after carbonization is higher than that of HCl-HCSs, and mesoporous pores are more abundant, indicating that NaOH-HCSs exposes more active sites and is more conducive to loading sulfonic acid groups.

Figure 9(a) shows the SEM image of the carbonized NaOH-HCSs after sulfonation with concentrated sulfuric acid (98%). Clearly, the sulfonated carbon spheres basically maintain a monodisperse spherical shape. A large amount of S exists on the surface of the sulfonated carbon spheres (Figure 9(b)), indicating that the sulfonic acid groups were successfully grafted onto the surface of the carbon spheres. After sulfonation, the diameter of carbon spheres further decreases. This is due to the dissolution or detachment of unstable substances remaining on the surface of carbon spheres during the sulfonation process; meanwhile, the sulfonation reaction leads to the break of weak binding parts on the surface of carbon spheres, ultimately resulting in a reduction in the diameter of carbon spheres [37].

Figure S2 shows the infrared spectra of NaOH-HCSs before and after carbonization and after sulfonation. Clearly, the peak of –OH at 3,471 cm⁻¹ and the peak of C=O at 1,700 cm⁻¹ in the carbonized carbon materials are weakened, while the peak of C=C at 1,600 cm⁻¹ is enhanced, indicating that the amounts of oxygen-containing functional groups are reduced and the carbonization degree is improved in the carbon materials after carbonization. After sulfonation, the characteristic peaks due to symmetric stretching of O=S=O and the stretching of SO₃ appear at 1,150 and 1,030 cm⁻¹, respectively [38].

Table S1 and Figure S3 show that the BET of NaOH-HCS after sulfonation increased from 183.04 to 201.37 cm²·g⁻¹, which is due to the small destruction on the carbon network producing the small particles. The decrease in pore

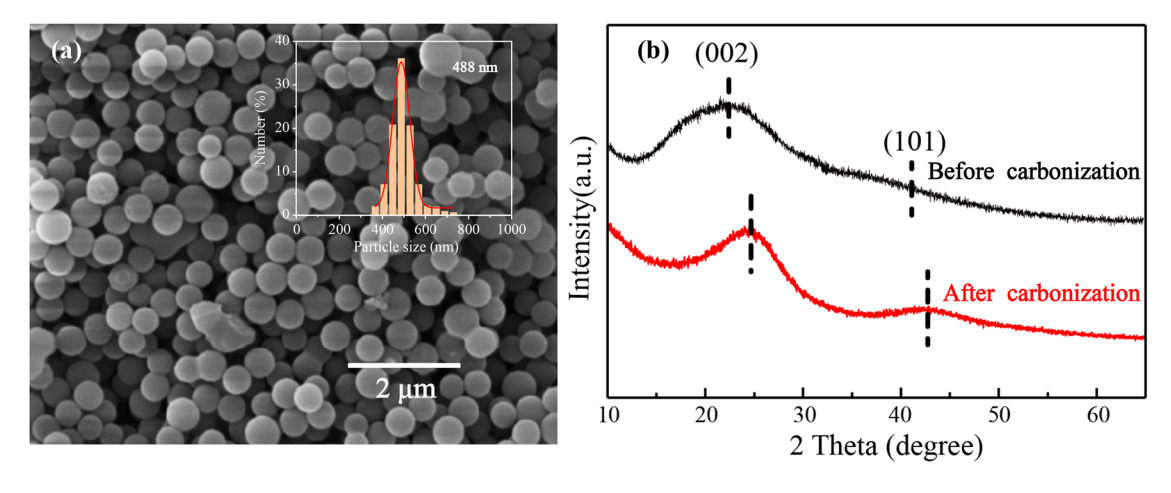


Figure 8: (a) SEM image of NaOH-HCSs after carbonization at 600°C and (b) XRD pattern before and after carbonization.

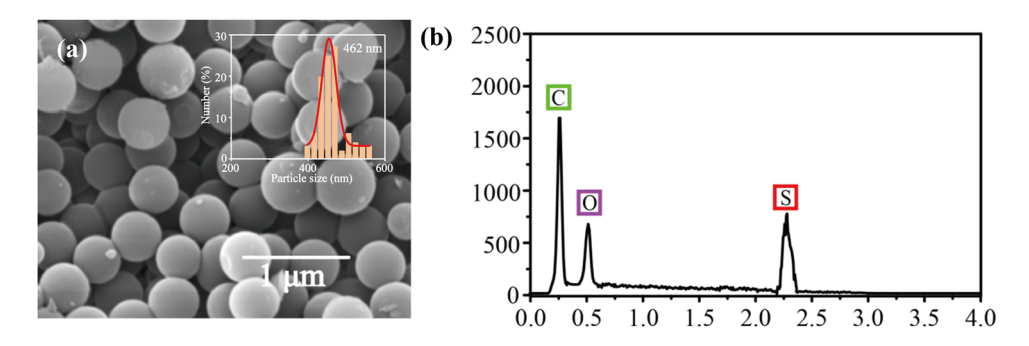


Figure 9: SEM image (a) and EDS spectrum (b) after sulfonation of NaOH-HCSs.

size after sulfonation suggests that the SO₃H groups were incorporated inside the pores of the carbon catalyst [39].

3.2.2 Application of carbon sphere-based solid acid catalysts in esterification reaction

BL is a novel bio-based cold flow improver for biodiesel fuels [40]. The addition of BL not only improves the lubricity and conductivity of diesels, but also reduces the particulate emissions in the diesel mixtures. Therefore, we selected the esterification reaction of LA and *n*-butanol to prepare BL as a probe reaction and investigated the activity and stability of the carbon sphere-based solid acid catalysts.

The amount of the catalyst plays an important role in esterification reactions. As the catalyst dosage increases from 1 to 10 wt%, the yield of BL rises from 24.34 to 93.15% (Figure 10(a)), which is because the increased number of reaction sites improves the esterification yield. The BL yield does not increase significantly when the catalyst dosage further increases to 15 wt%. The underlying reason may

be that because the excessive catalyst will aggregate, which reduces the contact with the reactants and makes a large number of active sites unavailable, resulting in little change in the BL yield. Figure 10(b) shows the effect of esterification temperature on the esterification rate. The esterification is accelerated with the temperature rise. The reason is that the esterification reaction is reversible and endothermic, and the temperature rise is conducive to the positive reaction. At 100°C, the yield of BL is up to 93.15%. With further increase of temperature, the BL yield increased to 96.36%, which does not increase significantly, indicating that 100°C is the optimal reaction temperature. The reproducibility of the solid acid catalysts was investigated under the optimal conditions. The catalysts were recovered, washed, and dried before the next experiment. The catalysts still have an esterification rate of 84.33% after five cycles (Figure 10(c)), indicating that the catalysts have high reproducibility. Carbon sphere-based solid acid catalysts are composed of polycyclic aromatic carbon sheets, and the inherent hydrophobicity of carbon prevents the hydration of -OH. Moreover, the -COOH in the catalysts increases the electron density between the

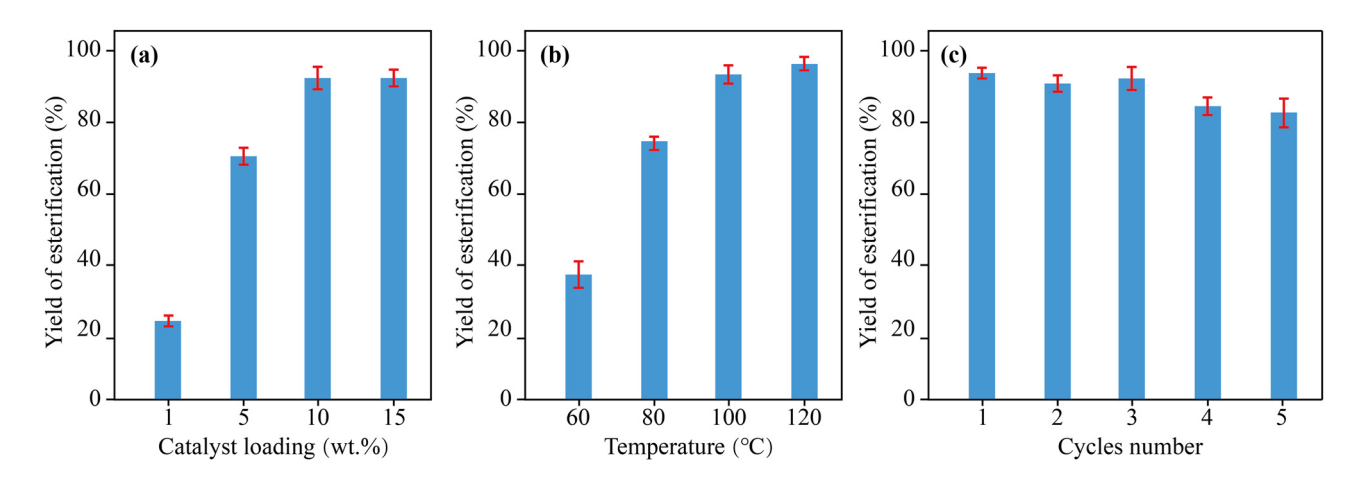


Figure 10: (a) effect of catalyst dosage on esterification rate, (b) effect of esterification temperature on esterification rate, and (c) catalyst stability test. Reaction conditions: 1.16 g of LA, 4.44 g of *n*-butanol, 3 h.

carbon and sulfur atoms, allowing -SO₃H to be tightly combined with the carbon skeleton, which accounts for the high cyclability of the catalysts.

4 Conclusions

In this study, the problem of low size uniformity of HCSs prepared by glucose-derived carbon spheres was reduced to a certain extent. The size uniformity of carbon spheres can be effectively improved by adding acid or base as catalysts. The particle size distribution of carbon spheres is the narrowest and the size is the smallest at pH 11. The reason is that the aldol reaction between cyclic ketones and aromatic ketones/aldehydes is more favorable in base systems, which accelerates the accumulation of aromatic clusters and the nucleation after reaching the critical supersaturation point. The shortened nucleation time significantly improves the uniformity of carbon spheres. Due to the limitation of raw materials, more raw materials are used for nucleation rather than nuclear growth, so the sizes of carbon spheres are smaller in base systems. NaOH-HCS-based solid acid catalysts were prepared by carbonization and sulfonation, and their application in biofuel catalysis was studied, expanding the application scope of carbon spheres.

Funding information: This study was supported by Technology Innovation Center for Land Engineering and Human Settlements, Shaanxi Land Engineering Construction Group Co. Ltd and Xi'an Jiaotong University (Grant Nos. 2024WHZ0231, 2021WHZ0093), the Shaanxi Provincial Land Engineering Construction Group Research Project (Grant Nos. DJNY DJNY-YB-2023-21, DJNY-ZD-2023-2, DJNY2024-28), and the Xi'an Science and Technology Plan Project (Grant No. 22NYYF028).

Author contributions: Lulu Zhang: writing-original draft, writing-review and editing, methodology; Jing Wang: writingreview and editing, formal analysis; Qingyi Wang: writing-original draft, writing-review and editing, conceptualization. All authors have accepted responsibility for the entire content of this manuscript and approved its submission.

Conflict of interest: The authors state no conflict of interest.

Data availability statement: The datasets generated during and/or analyzed during the current study are avail able from the corresponding author on reasonable request.

References

- Deshmukh, A. A., S. D. Mhlanga, and N. J. Coville. Carbon spheres. Materials Science and Engineering, R: Reports, Vol. 70, 2010, pp. 1–28.
- Cheng, X., C. Tang, C. Yan, J. Du, A. Chen, X. Liu, et al. Preparation of [2] porous carbon spheres and their application as anode materials for lithium-ion batteries: A review. Materials Today Nano, Vol. 22, 2023, pp. 100321-100356.
- Wei, Z., H. Ren, S. Wang, H. Qiu, X. Liu, and S. Jiang. Facile preparation of well dispersed uniform, porous carbon microspheres and their use as a new chromatographic adsorbent. Materials Letters, Vol. 105, 2013, pp. 144-147.
- [4] Xiong, W., H. Li, H. Wang, J. Yi, H. You, S. Zhang, et al. Hollow mesoporous carbon sphere loaded Ni-N₄ single-atom: support structure study for CO₂ electrocatalytic reduction catalyst. Small, Vol. 16, 2020, pp. 2003943-2003952.
- [5] Xiao, T., L. Zhao, H. Ge, M. Yang, W. Liu, G. Li, et al. Cobalt oxyhydroxide decorating hollow carbon sphere: A high-efficiency multi-functional material for Li-S batteries and alkaline electrocatalysis. Chemical Engineering Journal, Vol. 439, 2022, pp. 135790-135799.
- Ahn, S., K. Park, and K. Lee. Atomically dispersed Ru(III) on N-doped mesoporous carbon hollow spheres as catalysts for CO2 hydrogenation to formate. Chemical Engineering Journal, Vol. 442P1, 2022, pp. 136185-136193.
- Zhang, C., W. Zhang, X. Li, Z. Zhu, Q. Wang, S. Luo, et al. Honeycomb LaMnO_3 perovskite synthesized by a carbon sphere as a selfsacrificing template for supercapacitors. Energy & Fuels, Vol. 35, 2021, pp. 13457-13465.
- Réti, B., G. I. Kiss, T. Gyulavári, K. Baan, K. Magyari, and K. Hernadi. Carbon sphere templates for TiO₂ hollow structures: Preparation, characterization and photocatalytic activity. Catalysis Today, Vol. 284, 2017, pp. 160-168.
- Gong, Y., L. Xie, H. Li, and Y. Wang. Sustainable and scalable production of monodisperse and highly uniform colloidal carbonaceous spheres using sodium polyacrylate as the dispersant. Chemical Communications, Vol. 50, 2014, pp. 12633-12636.
- [10] Fu, J., T. Hui, D. An, W. Shan, G. Chen, S. Wageh, et al. Mesoporous biophotonic carbon spheres with tunable curvature for intelligent drug delivery. Nanophotonics, Vol. 11, 2022, pp. 5165-5175.
- Gui, X., Y. Chen, Z. Zhang, L. Lei, F. Zhu, W. Yang, et al. Fluorescent hollow mesoporous carbon spheres for drug loading and tumor treatment through 980-nm laser and microwave co-irradiation. Biomaterials, Vol. 248, 2020, pp. 120009-120018.
- [12] Cai, H., X. Lin, L. Tian, and X. Luo. One-step hydrothermal synthesis of carbonaceous spheres from glucose with an aluminum chloride catalyst and its adsorption characteristic for uranium(VI). Industrial & Engineering Chemistry Research, Vol. 55, 2016, pp. 9648-9656.
- Maruani, V., E. Framery, and B. Andrioletti. Influence of the ammonium salts used in the Bronsted acid catalyzed hydrothermal decomposition of D-glucose towards 5-HMF. New Journal of Chemistry, Vol. 22, 2020, pp. 4171-4176.
- Watanabe, M., Y. Aizawa, T. Iida, T. M. Aida, C. Levy, K. Sue, et al. Glucose reactions with acid and base catalysts in hot compressed water at 473 K. Carbohydrate Research, Vol. 340, 2005, pp. 1925-1930.

- [15] Mika, L., E. Cséfalvay, and Á. Németh. Catalytic conversion of carbohydrates to initial platform chemicals: chemistry and sustainability. Chemical Reviews, Vol. 118, 2018, pp. 505-613.
- [16] Kimura, H., M. Nakahara, and N. Matubayasi. In situ kinetic study on hydrothermal transformation of D-glucose into 5-hydroxymethylfurfural through D-fructose with ¹³C NMR. Journal of Physical Chemistry A, Vol. 115, 2011, pp. 14013-14021.
- [17] Qi, Y., B. Song, and Y. Qi. The roles of formic acid and levulinic acid on the formation and growth of carbonaceous spheres by hydrothermal carbonization. RSC Advances, Vol. 6, 2016, pp. 102428-102436.
- [18] Zhang, S., L. Zhang, L. Qian, J. Yang, Z. Ao, and W. Liu. Facile, sustainable and chemical-additive-free synthesis of monodisperse carbon spheres assisted by external pressure. ACS Sustainable Chemistry & Engineering, Vol. 7, 2019, pp. 7486-7490.
- [19] Lamer, V. and R. Dinegar. Theory production and mechanism of formation of monodispersed hydrosols. Journal of the American Chemical Society, Vol. 72, 1950, pp. 4847-4854.
- [20] Wohlgemuth, S. A., F. Vilela, M. M. Titirici, and M. Antonietti. A one-pot hydrothermal synthesis of tunable dual heteroatomdoped carbon microspheres. Green Chemistry, Vol. 14, 2012, pp. 741-749.
- [21] Yu, S., X. Dong, P. Zhao, Z. Luo, Z. Sun, X. Yang, et al. Decoupled temperature and pressure hydrothermal synthesis of carbon submicron spheres from cellulose. Nature Communications, Vol. 13, 2022, pp. 3616-3625.
- [22] Sobczuk, K. S., I. Pełech, U. Narkiewicz, P. Staciwa, D. Sibera, and D. Moszyński. The influence of the synthesis pH on the morphology and adsorption properties of carbon spheres. Applied Surface Science, Vol. 608, 2023, pp. 155196-155205.
- [23] Zhao, J., C. Zhou, C. He, Y. Dai, X. Jia, and Y. Yang. Efficient dehydration of fructose to 5-hydroxymethylfurfural over sulfonated carbon sphere solid acid catalysts. Catalysis Today, Vol. 608, 2023, pp. 155196-155205.
- [24] Mateo, W., H. Lei, E. Villota, M. Qian, Y. Zhao, E. Huo, et al. One-step synthesis of biomass-based sulfonated carbon catalyst by direct carbonization-sulfonation for organosoly delignification. Bioresource Technology, Vol. 319, 2021, pp. 124194-124200.
- [25] Gong, Y., Z. Wei, J. Wang, P. Zhang, H. Li, and Y. Wang. Design and fabrication of hierarchically porous carbon with a template-free method. Scientific Reports, Vol. 4, 2015, pp. 6349-6354.
- [26] Miao, Z. H., H. Wang, H. Yang, Z. Li, L. Zhen, and C. Y. Xu. Glucosederived carbonaceous nanospheres for photoacoustic imaging and photothermal therapy. ACS Applied Materials & Interface, Vol. 8, 2016, pp. 15904-15910.
- [27] Tongtummachat, T., N. Akkarawatkhoosith, A. Kaewchada, and A. Jaree. Conversion of glucose to 5-hydroxymethylfurfural in a microreactor. Frontiers in Chemistry, Vol. 7, 2020, pp. 951-957.

- [28] Titirici, M. and M. Antonietti. Chemistry and materials options of sustainable carbon materials made by hydrothermal carbonization. Chemical Society Reviews, Vol. 39, 2010, pp. 103-116.
- [29] Vashchenko, V., L. Kutulya, and A. Krivoshey. Simple and effective protocol for Claisen-Schmidt condensation of hindered cyclic ketones with aromatic aldehydes. Cheminform, Vol. 14, 2007, pp. 2125-2134.
- [30] Li, S., F. Liang, J. Wang, H. Zhang, and S. Zhang. Preparation of mono-dispersed carbonaceous spheres via hydrothermal process. Advanced Powder Technology, Vol. 28, 2017, pp. 2648-2657.
- [31] Zhang, Z., M. Qin, and B. Jia. Facile synthesis of novel bowl-like hollow carbon spheres by the combination of hydrothermal carbonization and soft templating. Chemical Communications, Vol. 53, 2017, pp. 2922-2925.
- [32] Chowdhury, Z. Z., B. Krishnan, S. Sagadevan, R. F. Rafique, N. Hamizi, Y. AbdulWahab, et al. Effect of temperature on the physical, electro-chemical and adsorption properties of carbon micro-spheres using hydrothermal carbonization process. Nanomaterials, Vol. 8, 2018, pp. 597-613.
- [33] Yang, J., G. Li, L. Zhang, and S. Zhang. Efficient production of *n*-butyl levulinate fuel additive from levulinic acid using amorphous carbon enriched with oxygenated groups. Catalysts, Vol. 8, 2018, pp. 14-25.
- [34] Li, M. and S. Liu. Hydrothermal synthesis, characterization, and KOH activation of carbon spheres from glucose. Carbohydrate Research, Vol. 346, 2011, pp. 999-1004.
- [35] Mohamed, S. K., M. Abuelhamd, N. K. Allam, A. Shahat, M. Ramadan, and H. Hassan. Eco-friendly facile synthesis of glucose-derived microporous carbon spheres electrodes with enhanced performance for water capacitive deionization. Desalination, Vol. 477, 2020, pp. 114278-114288.
- [36] Thommes, M., K. Kaneko, A. V. Neimark, J. P. Olivier, F. Rodriguez-Reinoso, J. Rouquerol, et al. Physisorption of gases, with special reference to the evaluation of surface area and pore size distribution (IUPAC Technical Report). Pure and Applied Chemistry, Vol. 87, 2015, pp. 1051-1069.
- [37] Ribeiro, F. C. P., J. L. Santos, R. O. Araujo, V. O. Santos, J. S. Chaar, J. Tenório, et al. Sustainable catalysts for esterification: Sulfonated carbon spheres from biomass waste using hydrothermal carbonization. Renewable Energy, Vol. 220, 2024, pp. 119653-119666.
- [38] Xu, C., R. Du, C. Yu, Z. Shi, J. Wang, and T. Li. Glucose-derived micromesoporous carbon spheres for high-performance lithium-sulfur batteries. Energy & Fuels, Vol. 37, 2023, pp. 1318-1326.
- [39] Lokman, I., U. Rashid, and Y. Taufiq-Yap. Meso- and macroporous sulfonated starch solid acid catalyst for esterification of palm fatty acid distillate. Arabian Journal of Chemistry, Vol. 9, 2016, pp. 179-189.
- [40] Tejero, M. A., E. Ramírez, C. Fité, J. Tejero, and F. Cunill Esterification of levulinic acid with butanol over ion exchange resins. Applied Catalysis A, Vol. 517, 2016, pp. 56-66.